Appl Phys A (2012) 106:131–136
DOI 10.1007/s00339-011-6640-5

Applied Physics A
Materials Science & Processing

Studying the luminescence efficiency of Lu_2O_3:Eu nanophosphor material for digital X-ray imaging applications

N. Kalyvas · P. Liaparinos · C. Michail · S. David · G. Fountos · M. Wójtowicz · E. Zych · I. Kandarakis

Received: 11 May 2011 / Accepted: 6 October 2011 / Published online: 5 November 2011

Abstract Scintillator materials are widely used in X-ray medical imaging detector applications, coupled with available photoreceptors like radiographic film or photoreceptors suitable for digital imaging like a-Si, charge-coupled devises (CCD), complementary metal-oxide-semiconductors (CMOS) and GaAs). In addition, scintillators can be utilized in non-medical imaging detectors such as industrial detectors for non-destructive testing (NDT) and detectors used for security purposes (i.e. airport luggage control). Image quality and dose burden in the above applications is associated with the amount of optical photons escaping the scintillator as well as the amount of optical photons captured by the photoreceptor. The former is characterized by the scintillator efficiency and the latter by the spectral matching between the emission spectrum of the scintillator and the spectral response of the photoreceptor. Recently, a scintillator material, europium-activated lutetium oxide (Lu_2O_3:Eu), has shown improved scintillating properties. Lu_2O_3:Eu samples of compact nanocrystalline non-agglomerated powder were developed in our laboratory using homogeneous precipitation from a water-toluene solution in the presence of polyvinyl alcohol as a surfactant. In order to test their light-emission properties, experimental measurements under the excitation of X-ray spectra with X-ray tube voltages between 50 kVp and 140 kVp were performed. This range of applied voltages is appropriate for X-ray radiology, NDT and security applications. Lu_2O_3:Eu was evaluated with respect to output yield and spectral compatibility of digital imaging photoreceptors (CCD-based, CMOS-based, amorphous silicon a:Si flat panels, ES20 and GaAs). High light yield and spectral compatibility increase the performance of the medical detector and reduce the dose burden to the personnel involved. In addition a theoretical model was used to determine the values for the Lu_2O_3:Eu optical photon light propagation parameters. The inverse diffusion length was found to be equal to 33 cm^2/g. In addition Lu_2O_3:Eu was found to match well with several photoreceptors capable of digital imaging (i.e. GaAs).

1 Introduction

Granular phosphor screens are powder layers which combine phosphor particles with a transparent binder material. These layers are used in indirect X-ray medical imaging detectors to transform the X-ray energy deposition to light information carries [1–3]. The phosphor grains, due to the high refractive index of phosphors compared with that of the binder, are highly scattering particles causing light diffusion within the screen, which in turn affects the final light output signal [4–7]. The optical effects of the phosphor screens in combination with the optical characteristics of the optical sensor, used to detect the emitted light, can provide useful medical information in terms of the sensitivity of the X-ray imaging system and the medical image brightness [2]. Image brightness can be estimated by evaluating the effective luminescence efficiency of the detector arising from the luminescence efficiency of the phosphor screen and its spectral compatibility (or the so-called matching factor) with the optical sensor [6, 7]. The former parameter expresses the

N. Kalyvas · P. Liaparinos · C. Michail · S. David · G. Fountos · I. Kandarakis (✉)
Department of Medical Instruments Technology, Technological Educational Institution of Athens, Ag. Spyridonos Street, Aigaleo, 122 10 Athens, Greece
e-mail: kandarakis@teiath.gr
Fax: +30-53-85302

M. Wójtowicz · E. Zych
Faculty of Chemistry, Wroclaw University, 14F Joliot-Curie Street, 50-383 Wroclaw, Poland

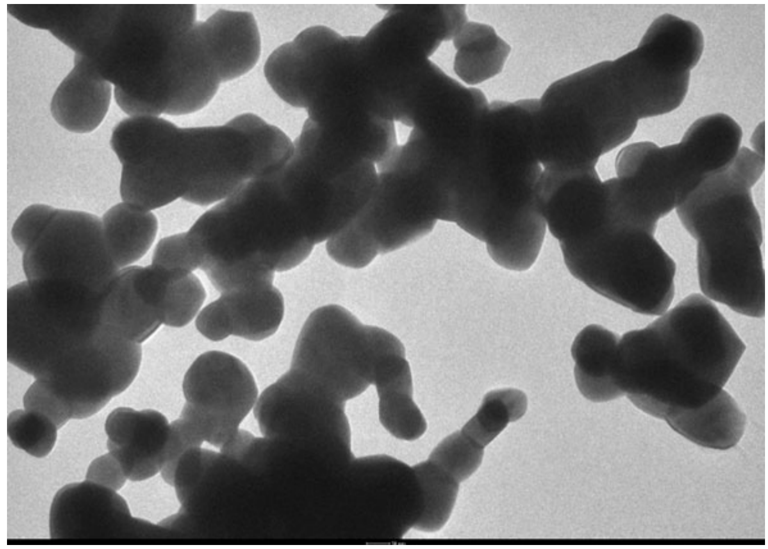

Fig. 1 The TEM image of Lu_2O_3:Eu nanoparticles. The scale corresponds to 50 nm

ability of the screen to produce light and the latter parameter expresses the ability of the optical sensor to capture the specific light wavelength emitted by the phosphor.

In this paper, we investigate the luminescence efficiency of Lu_2O_3:Eu. Lu_2O_3:Eu is a relatively new phosphor material, which is quite promising due to the following physical properties [8–13]: (a) high effective atomic number ($Z_{eff} = 63$), (b) high value of bulk density (9.4 g/cm^3), (c) peak light emission at 610 nm (red emission due to the Eu^{3+} activator) lying close to the maximum spectral sensitivity of electronic optical sensors (i.e. CCDs, amorphous silicon-a-Si:H sensors etc.) [14, 15]. Although this material exhibits intrinsic conversion efficiency relatively lower than that of Tb activated phosphors [12, 16, 17], a good spectral compatibility with suitable optical sensors could overcome this drawback. Thus, an investigation regarding the efficiency of Lu_2O_3:Eu under X-ray excitation combined with various optical sensors may be of interest for X-ray imaging applications. In addition a theoretical model [7, 18] was fitted to the experimental data in order to estimate the inverse diffusion length, which describes the optical photon losses as light propagates through the phosphor material.

2 Materials and methods

In the present article, the luminescence efficiency of europium activated lutetium oxide Lu_2O_3:Eu nanophosphor, developed in the form of compact powdered pills under X-ray excitation is investigated. Lu_2O_3:Eu samples of compact nanocrystalline non-agglomerated powder were developed precipitating lutetia hydroxides with urea from water-toluene solution heated up to about 80°C in the presence of polyvinyl alcohol (PVA) surfactant and some Li_2SO_4. After separation and washing the raw powder a thermal treatment at 1300°C for 5 hours was applied. A detailed description of the procedure is given in [E. Zych, J. Trojan-Piegza, and L. Kępiński, Homogeneously Precipitated Lu_2O_3:Eu Nanocrystalline Phosphor for X-ray Detection, *Sensor. Actuat. B-Chem* **109**, 112–118 (2005)] [19]. The reduced agglomeration, despite a high-temperature treatment, was achieved by synthetizing in a water solution with addition of SO_4^{2-} ions, which enter the product as a small impurity hindering the ability of the grains to growth and agglomerate. The percentage of Eu in the final solution was 5% [9]. In Fig. 1 the TEM image of Lu_2O_3:Eu grains is demonstrated. The luminescence efficiency plays a crucial role to detector sensitivity performance, which in turn is directly related to the principal physical properties of the phosphor material. The physical properties of Lu_2O_3:Eu are given in Table 1 [9, 11–13]. The luminescent efficiency of a scintillator (phosphor) based detector might be determined by two factors. First the X-ray absolute efficiency, which is the fraction of the emitted light photon power from the scintillator, per incident X-ray exposure. Second the spectral matching factor, which describes the fraction of emitted optical photon spectrum, which is detected by the photoreceptor. A high value of these two parameters can adequately reduce the radiation burden and increase the signal-to-noise ratio of the final image. The Lu_2O_3:Eu phosphor was investigated in the form of compact powder pills with surface densities of 222 mg/cm^2 and 468 mg/cm^2. As far as we know it is

Table 1 Physical and scintillating properties of Lu_2O_3:Eu

Density (g/cm^3)	9.4
Output yield	35000 photons/MeV
Effective atomic number	63
Emission peak (nm)	610
Index of refraction	2.1

the first time this kind of investigation was performed on ceramic nanophosphors in the form of compact powdered pills.

Absolute Luminescence Efficiency (AE)

The efficiency of the phosphor light output is affected by the intrinsic physical processes that take place within the screen. The contribution of these intrinsic processes can be expressed by the following relation [7, 18]:

$$AE = n_Q(E,T) n_C G_l(\sigma,\beta,\rho,T) \tag{1}$$

where $n_Q(E,T)$ is the fraction of the incident X-ray energy which is deposited in the phosphor material, n_C, is the intrinsic X-ray to light conversion efficiency giving the fraction of deposited X-ray energy transformed into light photon energy and $G_l(\sigma,\beta,\rho,T)$ is the light transmission efficiency, expressing the fraction of the light produced that reaches the screen output. σ, β and ρ are optical parameters related to light absorption, light scattering and light reflectivity in the phosphor material [5, 7, 18]. Assuming one-dimensional radiation transfer, AE can be described by a one-dimensional model for X-ray and light propagation in a phosphor screen [7, 18]:

$$\begin{aligned} AE = {}& \frac{n_C \gamma(E) t_r \mu(E)(1+\rho)e^{-\mu(E)T}}{2(\mu(E)^2-\sigma^2)} \\ & \times \frac{(\mu(E)-\sigma)(1-\beta)e^{-\sigma T}}{(1+\beta)(\rho+\beta)e^{\sigma T}-(1-\beta)(\rho-\beta)e^{-\sigma T}} \\ & + \frac{2(\sigma+\mu(E)\beta)e^{\mu(E)T}-(\mu(E)+\sigma)(1+\beta)e^{\sigma T}}{(1+\beta)(\rho+\beta)e^{\sigma T}-(1-\beta)(\rho-\beta)e^{-\sigma T}} \end{aligned} \tag{2}$$

where $\mu(E)$ is the X-ray energy mass absorption coefficient for X-ray energy E, $\gamma(E)$ is a conversion factor converting energy fluence (W/m^2) into exposure rate (mR/s), t_r is the transparency of the phosphor screen substrate and T is the surface density of the scintillator. If the energy spectrum of X-rays, $f(E)$, is to be taken into account, then AE can be calculated by summing over this spectrum, up to the peak energy (kVp) of the X-ray spectrum:

$$AE_{\mathrm{kVp}} = \frac{\sum_E f(E) AE}{\sum_E f(E)} \tag{3}$$

where kVp denotes the high voltage (kilovolt peak) applied to the X-ray tube. This voltage is equal to the maximum energy of the X-ray spectrum.

Lu_2O_3:Eu phosphor—optical sensors combinations

Spectral compatibility expresses the ability of the optical sensor to capture the specific light wavelength emitted by the phosphor screen, and is often estimated by the spectral matching factor a_s, which is defined as follows [20, 21]:

$$a_s = \frac{\int_{\lambda_1}^{\lambda_2} S_P(\lambda) S_D(\lambda)\, d\lambda}{\int_{\lambda_1}^{\lambda_2} S_P(\lambda)\, d\lambda} \tag{4}$$

where $S_p(\lambda)$ is the spectrum of the emitted light, $S_D(\lambda)$ is the spectral sensitivity of the optical photon detector and λ denotes light wavelength. The spectral compatibility of Lu_2O_3:Eu phosphor was assessed with various optical detectors that could be utilized in digital X-ray imaging applications, as given by: (a) charge-coupled device (CCD) with: (i) broadband AR coating, (ii) IR AR coating, (iii) traditional polygates, (iv) ITO gates, (v) ITO gates with micro-lenses, (vi) traditional polygates LOD, (vii) no polygates LOD, (b) complementary metal-oxide-semiconductor (CMOS) such as: (i) monolithic CMOS 0.25 μ, (ii) hybrid CMOS with NIR AR coating, (iii) hybrid CMOS with Blue AR coating, (iv) photogate array (0.5 μm PGATE), (c) Si-based photodiodes, such as: c-Si and Si photodiode S1227BR and (d) GaAs and ES20 photocathodes. The sensitivity curves of the optical sensors were taken from the literature [14, 21].

2.1 The experimental method

The scintillating screens were irradiated by X-rays at various tube voltages (from 50 to 140 kV) employing a Del Medical Eureka X-ray radiographic unit with 1.5 mm Al inherent tube filtration. Tube voltage and incident exposure rate measurements were performed using a Victoreen 4000M ionization chamber. An additional 20 mm Al filtration was introduced in the beam to simulate an average human body. Absolute efficiency was determined by measuring the light energy flux emitted by the irradiated screen and dividing by the incident exposure rate, measured at screen position. The experimental set-up for light energy fluence measurements comprised a photomultiplier (EMI 9798 B) with an extended sensitivity S20 photocathode and enclosed within a bronze light tight chamber [6, 7, 18]. The output current was amplified and finally measured by a vibrating reed (Cary 400) electrometer operated in current mode. An analogue to digital converter was employed to digitize electrometer's output, which was then stored on a computer. The absolute efficiency was then computed from electrometer's output current and dosimeter data by performing conversions and corrections according to the formula [6, 7, 18]

$$AE = \frac{i_{\mathrm{elec}}(pA)}{S n_p a_s c_g} \frac{1}{X} \tag{5}$$

where i_{elec} is the electrometer's output current in pA, S is the area of the irradiated screen and n_p is the photocathode's peak photosensitivity expressed in mA/W. a_s is the spectral compatibility factor expressing the compatibility of the scintillator's emission spectrum to the spectral sensitivity of the photocathode (extended S20). a_s was determined by (4). The spectral sensitivity of the photodetector (photocathode), was obtained from the manufacturers datasheet. c_g is the geometric light collection efficiency of the experimental set-up, expressing the fraction of screen's emitted light incident

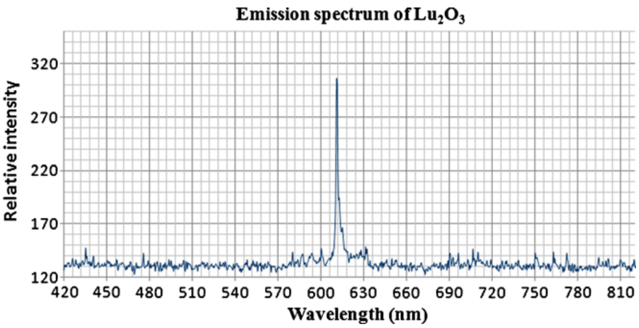

Fig. 2 Emitted light spectrum of Lu_2O_3:Eu phosphors

on the photocathode. This fraction has been determined by taking into consideration: (a) the angular distribution of the light emitted by the screen, which was obtained from literature and (b) the distance between the screen and the photocathode. Finally X, in (5), is the measured incident X-ray exposure rate.

In order to measure the optical spectral distribution, $S_p(\lambda)$of Lu_2O_3:Eu, the scintillator was excited with a UV source. $S_p(\lambda)$ was obtained by means of an Oriel 7240 grating monochromator. These data were corrected for the optical response of the monochromator, the UV energy and the background, in order to diminish any systematic errors in $S_p(\lambda)$ calculations. The measured emitted optical spectrum of Lu_2O_3:Eu is demonstrated in Fig. 2, with a peak value at 610 nm, in accordance with other published results [9, 11, 13].

3 Results and discussion

Figures 3a and 3b show the variation of experimental absolute luminescence efficiency of Lu_2O_3:Eu scintillator with increasing X-ray tube peak voltage. The experimental *AE* values were determined by means of (5) and they are expressed in efficiency units (EU, 1 EU = 1 $\mu W\, m^{-2}$/mR). It can be observed that increasing tube voltage raise the absolute efficiency for tube voltages up to 90 kVp and up to 120 kVp for the 222 mg/cm^2 and the 468 mg/cm^2 phosphors, respectively. At higher X-ray energies AE is almost constant. This occurs because at higher energies the depth of X-ray interaction increases and the optical photons are created closer to the phosphor's emitting surface. Therefore the fraction of escaping optical photons is larger. On the other hand the number of optical photons produced at lower kVp is larger, due to the higher X-ray absorption at lower energies. Thus the shape of the absolute efficiency curve is affected by the combined effect of X-ray absorption in the phosphor and the optical photon escape to the output. The AE values of Lu_2O_3:Eu are lower than commercially available Tb activated phosphors (i.e. Gd_2O_2S:Tb) and lower or comparable with other Eu activated phosphors (i.e. Gd_2O_2S:Eu, Y_2O_3:Eu) [6, 22]. All the aforementioned phosphors, however, had common grain size (5 µm to 12 µm) and were constructed in thinner phosphor screens (less than 150 mg/cm^2) using different techniques, thus a larger amount of optical photons created in the phosphor mass could escape to the output. It could be of great interest if the methodology for Lu_2O_3:Eu compact screens, used in this work, could be used to construct screens of surface densities smaller than 150 mg/cm^2. In addition Lu_2O_3:Eu was found better than Ce activated phosphors like YAP:Ce and YAG:Ce [7–18].

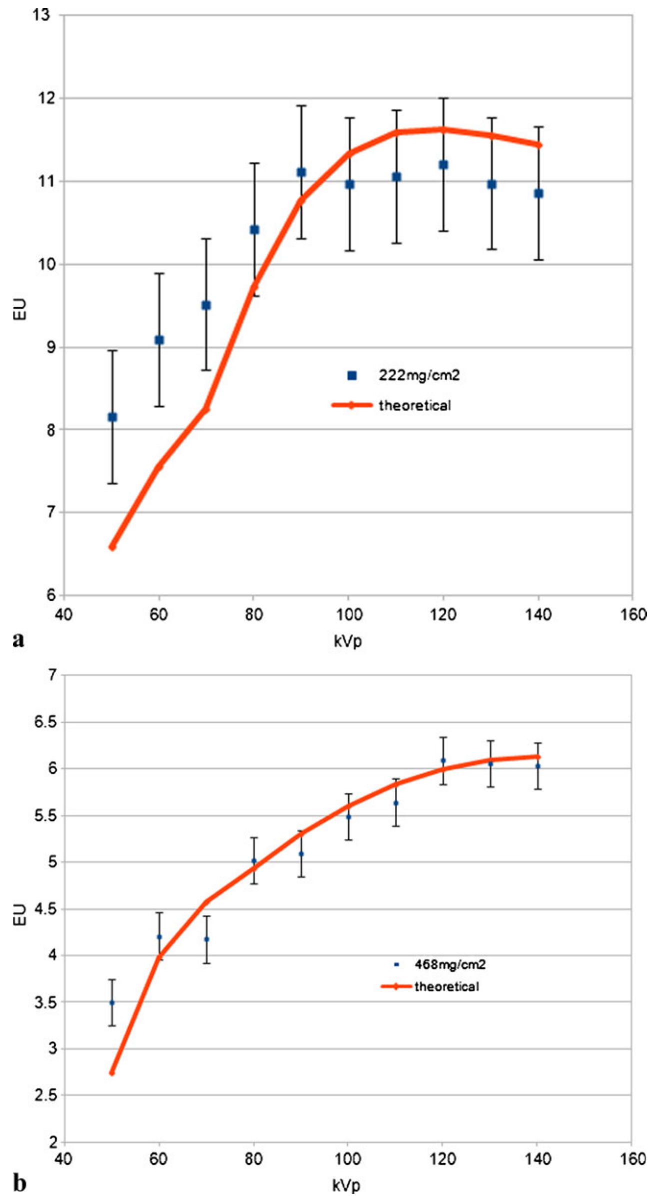

Fig. 3 The variation of experimental and theoretical absolute luminescence efficiency of 222 mg/cm^2 (**a**) and 468 mg/cm^2 (**b**) Lu_2O_3:Eu scintillator with increasing X-ray tube peak voltage

Table 2 Matching factors between Lu_2O_3:Eu phosphor material with various optical sensors

Photoreceptor	Matching factor
CMOS 0.5 µm Pgate	0.12
Hybrid CMOS with NIR AR Coating	0.81
Hybrid CMOS with BLUE AR Coating	0.81
Monolithic 0.25 µm CMOS-Image sensor	0.46
c-Si	0.56
Si photodiode S1227BR	0.81
GaAs	0.94
ES20	0.75
CCD FF-no LOD	0.26
CCD Ffwith LOD	0.17
CCD BI With Broadband AR coating	0.64
CCD BI With IR AR coating	0.65
CCD with ITO gates	0.41
CCD with poly gates	0.28
CCD with ITO gates&μlens	0.58

In order to theoretically investigate the response of Lu_2O_3:Eu and determine the parameters related to optical photon propagation to the output, (2) and (3) was used to fit the experimental data. The fitting was performed by first selecting appropriate values for the parameters t_r, ρ and β obtained by our previous studies ($t_r = 1$, $\rho = 0.9$ and $\beta = 0.03$). The value t_r was chosen one since no optical substrate was present. The value of n_C was taken equal to 0.08 [12]. The value of σ was determined by fitting (2) to the experimental data by trial and error method. Best fit was found for σ equal to 33 cm^2/g. The theoretical absolute efficiency values are also demonstrated in Fig. 3a and Fig. 3b. The value of σ found in this way is higher than the values reported for other Eu activated phosphors (i.e. YVO_4:Eu and Y_2O_3:Eu with σ ranges between 20 and 26 cm^2/g) and is closer to values reported for Tb activated green emitting phosphors (i.e. Gd_2O_2S:Tb, La_2O_2S:Tb with ranges between 30 cm^2/g and 40 cm^2/g) [22–25]. However, these phosphors were composed of grains well above the nanoparticle range (some microns) and were examined in the form of phosphors screens prepared with the sedimentation technique. As far as we know it is the first time this theoretical model was applied to nanophosphors investigated in the form of compact powdered pills. So the value of $\sigma = 33$ cm^2/g corresponds to the combined effect of the grain size and the screen preparation technique. A high value of σ is generally corresponding to macroscopically higher scatter and absorption in the phosphor screen [7, 26].

In Table 2, the spectral compatibility between the optical spectra emitted by Lu_2O_3:Eu phosphor and the sensitivity of optical detectors that can be used in medical, NDT or security applications are given. It can be observed that Lu_2O_3:Eu can be used with various photoreceptors such as Hybrid CMOS with NIR AR Coating, Hybrid CMOS with BLUE AR Coating, Si photodiode S1227BR, and GaAs, which demonstrate a matching factor above 0.8. It must be noted that a high value of a_s reduces the radiation burden (of the patient and the X-ray equipment operators in medical and other applications) and increases the signal-to-noise ratio of the detector since the number of detected optical photons per X-ray are increased.

4 Conclusion

The purpose of the present study was the evaluation of the X-ray luminescence efficiency and optical related parameters of Lu_2O_3:Eu nanophosphor material, constructed in the form of compact pills, for use in X-ray digital detectors. The X-ray luminescence efficiency was estimated by using experimental techniques for X-ray imaging applications. Lu_2O_3:Eu phosphor exhibits lower light emission properties than Tb activated phosphors, its response is, however, comparable or better than other Eu and Ce activated phosphors, respectively. The inverse diffusion length of the phosphor screens under consideration was calculated as 33 cm^2/g. In addition the present study showed that Lu_2O_3:Eu can be combined with photoreceptors capable for digital imaging such as GaAs, Hybrid CMOS with NIR AR Coating, Hybrid CMOS with BLUE AR Coating and Si photodiode S1227BR.

References

1. J.A. Rowlands, J. Yorkston, Flat panel detectors for digital radiography, in *Handbook of Medical Imaging*, ed. by J. Beutel, H.L. Kundel, R.L. Van Metter. Physics and Psychophysics, vol. 1 (SPIE Press, Bellingham, 2000), pp. 223–328
2. A. Del Guerra, *Ionizing Radiation Detectors for Medical Imaging* (World Scientific, Singapore, 2004). ISBN 9812386742
3. M.J. Yaffe, J.A. Rowlands, Phys. Med. Biol. **42**, 1 (1997)
4. P. Liaparinos, I. Kandarakis, D. Cavouras, H. Delis, G. Panayiotakis, Med. Phys. **33**, 4502 (2006)
5. R.M. Nishikawa, M.J. Yaffe, Med. Phys. **17**, 894 (1990)
6. C. Michail, G. Fountos, P. Liaparinos, N. Kalyvas I. Valais, I. Kandarakis, G. Panayiotakis, Med. Phys. **37**, 3694 (2010)
7. N. Kalivas, I. Valais, D. Nikolopoulos, A. Konstantinidis, A. Gaitanis, D. Cavouras, C.D. Nomicos, G. Panayiotakis, I. Kandarakis, Appl. Phys. A **89**, 443 (2007)
8. P. Liaparinos, I. Kandarakis, Med. Phys. **36**, 1985 (2009)
9. E. Zych, A. Meijering, C. de Mello Donega, J. Phys., Condens. Matter **15**, 5145 (2003)
10. E. Zych, J. Trojan-Piegza, D. Hreniak, W. Strek, J. Appl. Phys. **94**, 1318 (2003)
11. A. Lempicki, C. Brecher, P. Szupryczynski, H. Lingertat, V.V. Nagarkar, S.V. Tipnis, S.R. Miller, Nucl. Instrum. Methods Phys. Res., Sect. A, Accel. Spectrom. Detect. Assoc. Equip. **488**, 579 (2002)
12. M. Nikl, Meas. Sci. Technol. **17**, R37 (2006)

13. V.V. Nagarkar, S.R. Miller, S.V. Tipnis, A. Lempicki, C. Brecher, H. Lingertat, Nucl. Instrum. Methods Phys. Res., Sect. B, Beam Interact. Mater. Atoms **213**, 250 (2004)
14. P. Magnan, Nucl. Instrum. Methods Phys. Res., Sect. A, Accel. Spectrom. Detect. Assoc. Equip. **504**, 199 (2003)
15. S.M. Gruner, M.W. Tate, E.F. Eikenberry, Rev. Sci. Instrum. **73**, 2816 (2002)
16. R.H. Bartram, A. Lempicki, L.A. Kappers, D.S. Hamilton, J. Lumin. **106**, 169 (2004)
17. G. Blasse, J. Lumin. **60&61**, 930 (1994)
18. D. Cavouras, I. Kandarakis, D. Nikolopoulos, I. Kalatzis, G. Kagadis, N. Kalivas, A. Episkopakis, D. Linardatos, M. Roussou, E. Nirgianaki, D. Margetis, I. Valais, I. Sianoudis, K. Kourkoutas, N. Dimitropoulos, A. Louizi, C. Nomicos, G. Panayiotakis, Appl. Phys. B **80**, 923 (2005)
19. E. Zych, J. Trojan-Piegza, L. Kępiński, Sens. Actuators B, Chem. **109**, 112 (2005)
20. G.E. Giakoumakis, Appl. Phys. A **52**, 7 (1991)
21. N. Kalivas, L. Costaridou, I. Kandarakis, D. Cavouras, C.D. Nomicos, G. Panayiotakis, Appl. Phys. A **78**, 915 (2004)
22. D. Cavouras, I. Kandarakis, G.S. Panayiotakis, E. Evangelou, C.D. Nomicos, Med. Phys. **23**, 1965 (1996)
23. I. Kandarakis, D. Cavouras, Eur. Radiol. **11**, 1083 (2001)
24. I. Kandarakis, D. Cavouras, G.S. Panayiotakis, C.D. Nomicos, Phys. Med. Biol. **42**, 1351 (1997)
25. I. Kandarakis, D. Cavouras, E. Kanellopoulos, C.D. Nomicos, G.S. Panayiotakis, Radiat. Meas. **29**, 481 (1998)
26. H.C. Van de Hulst, *Light Scattering by Small Particles* (Wiley, New York, 1957)